Bull. Mater. Sci. (2020) 43:186
https://doi.org/10.1007/s12034-020-02162-y

Hydrophobic recovery of cross-linked polydimethylsiloxane films and its consequence in soft nano patterning

NANDINI BHANDARU[1,2], NEHA AGRAWAL[1], MENEKA BANIK[1], RABIBRATA MUKHERJEE[1,*] and ASHUTOSH SHARMA[3]

[1]Instability and Soft Patterning Laboratory, Department of Chemical Engineering, Indian Institute of Technology Kharagpur, Kharagpur 721302, India
[2]Department of Chemical Engineering, BITS Pilani, Hyderabad Campus, Hyderabad 500078, India
[3]Department of Chemical Engineering, Indian Institute of Technology Kanpur, Kanpur 208016, India
*Author for correspondence (rabibrata@che.iitkgp.ac.in)

MS received 4 September 2019; accepted 4 January 2020; published online 8 August 2020

Abstract. Cross-linked polydimethylsiloxane (PDMS) films and surfaces obtained by thermal cross-linking of commercially available Sylgard 184 are widely utilized in many areas of science, due to superior thermal stability, low dielectric constant, transparency and biocompatibility. Cross-linked PDMS surfaces are weakly hydrophobic and several experiments, particularly the ones that utilize capillary-driven microscale flow require the modulation of the surface wettability. A well-known strategy to achieve the same is by exposing the Sylgard 184 surface to UV/ozone (UVO) treatment at room temperature. Depending on the duration of exposure, the wettability drops from hydrophobic to a near-complete wetting (water contact angle $\sim 10°$), due to the formation of a surface oxide layer. However, under normal atmospheric conditions, these surfaces recover their hydrophobicity over a period of time due to diffusive migration of the uncrosslinked oligomers to the surface, and formation of a hydrophobic dimethyl silicone layer. We explore the hydrophobic recovery process as a function of cross-linker concentration and UVO exposure time and show how a partially or fully recovered PDMS stamp may influence subsequent nanopatterning, including the possible creation of features with different morphology using a single stamp.

Keywords. PDMS; hydrophobicity; UVO exposure; soft lithography; patterning.

1. Introduction

Sylgard 184 [1] or cross-linked poly(dimethylsiloxane) (PDMS) is a thermo-curable elastomer which finds application in various areas such as coatings [2], gas separation membranes [3], biochips [4], templates for cell adhesion [5] and so on, due to unique properties, including easy and cost-effective moulding [6] with possible modulation of stiffness [7]. It is widely used as a stamp or master in soft lithography techniques, by which it is possible to create a perfect negative replica of the stamp on different types of materials that include glassy polymers [8], inorganic sol–gel films etc. [9]. Crosslinked PDMS stamps are also essential for microcontact printing for making chemically patterned surfaces [10,11], and Janus colloids [12]. Crosslinked PDMS stamps are fabricated by replica moulding against a lithographically fabricated master [13–17]. Crosslinked PDMS is also widely used for the fabrication of microchannels [18], including those with twisted geometry [19] and internal patterns [20]. Crosslinked PDMS thin films are unique model systems for studying adhesion and debonding of soft surfaces [21,22], including studying elastic contact instability with a flat [23] or patterned stamp [24,25], and under the influence of an externally applied electric field [26,27]. Thermocurable PDMS-based moulding is also absolutely essential in reproducing complex biomimetic structures from actual biological entities such as gecko feet, lotus leaf, rose petal and so on [28].

The surface of PDMS is weakly hydrophobic, exhibiting an equilibrium water contact angle (WCA) $\approx 106°$. This often makes it difficult to engender flow inside PDMS microchannels with aqueous solutions and also makes it difficult to obtain a thin film on it by spin coating due to the non-wettability of the surface [29]. Another problem that arises due to the high hydrophobicity of PDMS is that it absorbs organic solvents and hydrophobic analytes, causing fouling of the material [30]. In contrast, a wettable PDMS surface offers great advantages including reduced nucleation of air bubbles in microfluidic channels [31]. A hydrophilic PDMS stamp allows microcontact printing of hydrophilic polymers and proteins [32]. A hydrophilic surface also improves its bonding ability to dissimilar materials while producing no change in the bulk properties.

To properly adjust the surface characteristics of PDMS, it is important to understand the changes that the PDMS surface undergoes when exposed to various surface treatments. Various surface modification methods for PDMS have been reported in the literature, which includes silanization, adsorption of polymers or proteins, layer-by-layer deposition, sol–gel coatings, lipid coatings etc. [33,34]. However, most of these techniques suffer problems such as non-uniform surface properties and difficulties in scaling up. To circumvent the limitations, traditionally PDMS surfaces have been modified by exposure to energy sources such as oxygen plasma [35], ultraviolet light [36] and corona discharge [37], as they alter the surface property effectively, conveniently and uniformly over large areas. In the presence of an energy source, the non-polar groups (mainly $-CH_3$) present on the surface are substituted with the polar groups (mainly –OH), resulting in surface oxidation of the PDMS surface [38,39].

Of all the available techniques reported in the literature, UV-ozone-mediated surface oxidation is an extremely facile technique, since it uses far less energy than oxygen plasma [40], and requires simpler infrastructure. Though the change in wettability of the PDMS surface by UV-ozone treatment is much slower as compared to oxygen plasma exposure [41], this feature can be advantageously used for precisely tailoring the wettability of the PDMS surface more effectively with greater control. However, it turns out that the hydrophilicity of the UVO-modified PDMS surfaces gradually reduce with time, which was first reported by Owen and co-worker [39], and is attributed to the migration of uncrosslinked PDMS chains to the surface with time [42,43]. Recently, Senzai and Fuzikawa [44] reported that low-molecular-weight cyclic siloxane derivatives evaporated from the PDMS film itself, which get re-chemisorbed on oxygen-plasma-induced oxidized surfaces leading to hydrophobic recovery and was ascribed to the ring-opening of the cyclic siloxane derivatives by functional groups generated from substrate surface oxidation.

Despite available literature on the hydrophobic recovery of PDMS surfaces, systematic investigations of time-dependant recovery particularly as a function of the initial cross-linked concentration and duration of UVO exposure, as well as its consequences on possible patterning applications have never been explored before and are reported for the first time in this paper. Apart from reporting the variation of WCA as a function of time, we also show how topographically patterned PDMS stamps, UVO exposed for different time durations can be used for obtaining different patterns on a glassy polymer polystyrene (PS) film. We show that it becomes possible to create patterns on the surface of the PS film, which are not a mere negative replica of the original stamp pattern, by using stamps of different wettability in a single step. It is worth highlighting that creating a non-negative replica by imprinting, which is also known as 'patterning beyond the master' is a difficult concept and has been achieved only in handful of cases based on complex phenomena such as stress relaxation [45], adhesion–debonding hysteresis of soft films [46] and so on. Finally, we show that with UVO exposed PDMS surfaces, it also becomes possible to pattern another PDMS layer or film in one step, which is extremely important in creating positive biomimetic replicas and has so far been achieved by complex techniques involving several intermediate steps [47,48]. We show that the capability of patterning a PDMS layer with a UVO exposed PDMS stamp decreases with progressive hydrophobic recovery.

2. Materials and methods

2.1 *Sylgard 184 flat and patterned stamps*

Flat and patterned films of Sylgard 184, a two-part thermocurable PDMS elastomer (Dow Corning, USA), was created by spin coating on a cleaned glass slide. The composition of part A oligomer is a combination of vinyl terminated siloxanes (dimethyl-vinyl terminated dimethylsiloxane) and tetra(trimethylsiloxy)silane. The curing agent (part B) is a dimethyl, methyl hydrogen siloxane [1]. The oligomer (part B) to the cross-linker (part A) ratio (CL%) was maintained at 10% (w/w). For certain samples, the CL% was taken as 5 and 15% to study the effect of the cross-linker fraction on hydrophobic recovery. The mixture of parts A and B was degassed and then diluted in *n*-heptane at a ratio of 1:4 (v/v) for spin coating. The film thickness in all samples was ≈ 10 μm, measured using the weight difference method. The film was kept in a vacuum oven at 30°C for 2 h and then cured at 120°C for 12 h for complete crosslinking of the polymer. A uniform soft solid block of Sylgard 184 was formed on the glass slide. Thickness was also varied by changing the dilution of the casting solvent in certain cases.

Patterned Sylgard 184 stamps were created by the method of replica moulding (REM) against the polycarbonate part of commercially available optical compact discs, which contains parallel tracks. The patterns consist of a line and groove geometry with periodicity, $\lambda_P = 1.5$ μm, line width, $l_P = 750$ nm and stripe height, $h_P = 120$ nm [24]. The cross-patterned stamps were created by REM of the Sylgard film against a lithographically fabricated stamp [49].

2.2 *UV-ozone treatment*

Both flat and patterned stamps of Sylgard 184 were exposed to UV-ozone (UVO) treatment in a UVO chamber (PSD Pro UV−O, Novascan, USA). The samples were treated for different durations of time (t_E) from 0 to 120 min. UV irradiation at a wavelength of 184.9 nm dissociates molecular oxygen into atomic oxygen, which recombines with the molecular oxygen to produce ozone. The ozone further gets dissociated by the 253.7 nm UV−C irradiation

resulting in the formation of atomic oxygen, which reacts with the siloxane groups present on the substrate surfaces.

2.3 *Contact angle measurements*

The WCA of the surface-modified substrates was measured using contact angle goniometer (Model 290, Ramè-hart Instruments Co., USA) based on static contact angle measurements. The tangent placed at the intersection of the drop and the slide surface when the drop had reached a 'metastable equilibrium' (the process of spreading of the drops) offered the WCA measurement. The values were obtained by the 'circle method' used by the DROPImage software provided along with the goniometer and the reported data is the mean of the tangents taken at both sides of each droplet. An average of at least three measurements was determined at different positions of the substrate. Further, the surface energies of different stamps were calculated from Owen's equation using water, ethylene glycol and toluene as probing liquids. Flat Sylgard 184 block without UVO treatment has surface energy, $\gamma_{uvo} = 24.2$ mJ m^{-2} [38]. The temperature and relative humidity in all measurements were kept constant at 26°C and 35%, respectively.

2.4 *Polystyrene film preparation and patterning*

The patterned Sylgard 184 stamps UVO exposed for different duration were used to patterning polymer thin films. Thin films of polystyrene (PS, MW: 280K, PDI: 1.03, Sigma, UK) were spin-coated (Apex Instruments, India) from its dilute solution in toluene (HPLC grade, Merck India) onto cleaned polished quartz pieces (15 mm × 15 mm, Applied Optics, India). A solution with a polymer concentration of 1.5% (w/v) was coated at 2500 RPM for 60 s to obtain films with a thickness (h_F) ≈ 65nm. These films were heated in a vacuum oven for 3 h at 60°C for residual solvent removal. The PS films were then patterned with the patterned Sylgard-184 stamps. The stamps were placed on the PS thin films and a transient uniform load of 4 kPa was applied to ensure complete conformal contact. After removal of the load, the assembly was kept inside a vacuum oven and annealed in the presence at 160°C for 4 h. The temperature chosen was significantly higher than the glass transition temperature of PS (T_g = 105°C) to ensure mould filling by the viscous polymer. After cooling to room temperature, the stamp was peeled off, and the replicated patterns on PS were analysed under an atomic force microscope (AFM) (5100, Agilent Technologies).

3. Results and discussion

UVO treatment is relatively mild energy-mediated surface treatment, which causes significant changes in the surface and near-surface properties of Sylgard 184, though the bulk properties remain unchanged. PDMS gets oxidized under UVO irradiation primarily due to the action of UV corresponding to two different wavelengths: 184.9 and 253.7 nm [41]. The CH_3 groups of the PDMS side chains on the surface are eliminated by the reaction with ozone in the presence of 253.7 nm UV. Initial oxidation involves the incorporation of the polar groups (Si-OH), which get attached covalently to the exposed surfaces of Sylgard 184 by replacing the Si-CH_3 linkages [18,41,50]. Gradually, on prolonged oxidation (longer t_E), a hydrophilic ceramic silica-like stiff layer (SiO_x) is formed on the Sylgard surface [41]. This layer alters the surface wettability, rendering it hydrophilic. The layer also acts as a diffusion barrier and prevents solvent swelling of Sylgard 184 films and surfaces [51].

The variation in the wettability of a crosslinked PDMS surface as a function of UVO exposure time is shown in figure 1a. Our measurements revealed that flat Sylgard 184 block exhibits WCA ≈ 108.6° ± 2.2° before UVO exposure. From figure 1a it can be seen that the drop in contact angle is marginal and the surface retains its hydrophobicity till exposure time t_E ≈ 60 min. After that, there is a rapid drop in WCA to values as low as 8.8° (almost a state of complete wetting), as t_E increases to 90 min. Exposure for longer duration does not change the wettability of the surface any further. The UVO oxidation process, which makes the Sylgard 184 surface hydrophilic, competes with the migration of low molecular weight (LMW) species towards the surface, which makes the surface hydrophobic. Thus, the existence of a large amount of LMW species weakens the efficiency of UVO oxidation [52] and is responsible for the very sluggish initial change in wettability for $t_E \leq 60$ min. Figure 1b–d shows the AFM scans of the Sylgard 184 surfaces before and after UVO exposure for different t_E. For all the surfaces, the root mean square (RMS) roughness is ∼0.3 nm. This reveals that the Sylgard 184 surface remains reasonably flat with no apparent change in surface roughness upon UVO exposure. At lower t_E, the extent of oxidation is low and consequently, the SiO_x layer formed is not rigid and remains conformal with the softer unexposed Sylgard layer below. However, figure 1c and d reveals the appearance of nano-sized holes on the surface of the oxide layer, which marginally grows in size with t_E.

It is argued that the main reasons for hydrophobic recovery of UVO exposed PDMS film are the diffusion of the LMW, uncrosslinked PDMS molecules from the bulk of the film to the surface and overturning of the surface polar hydrophilic groups (Si-OH or Si-CH_2OH) [53]. With longer t_E, the number of methyl groups on the surface decreases and the SiO_x formation increases and makes the oxide layer rigid. The mismatch in the elastic modulus of the stiff oxide layer and the bulk PDMS leads to interfacial mechanical stress, which is responsible for the formation of the nanoscale cracks on the surface of the oxide layer [42], as can be seen in figure 1d. In samples exposed for longer t_E, the presence of the cracks favours the diffusion of the

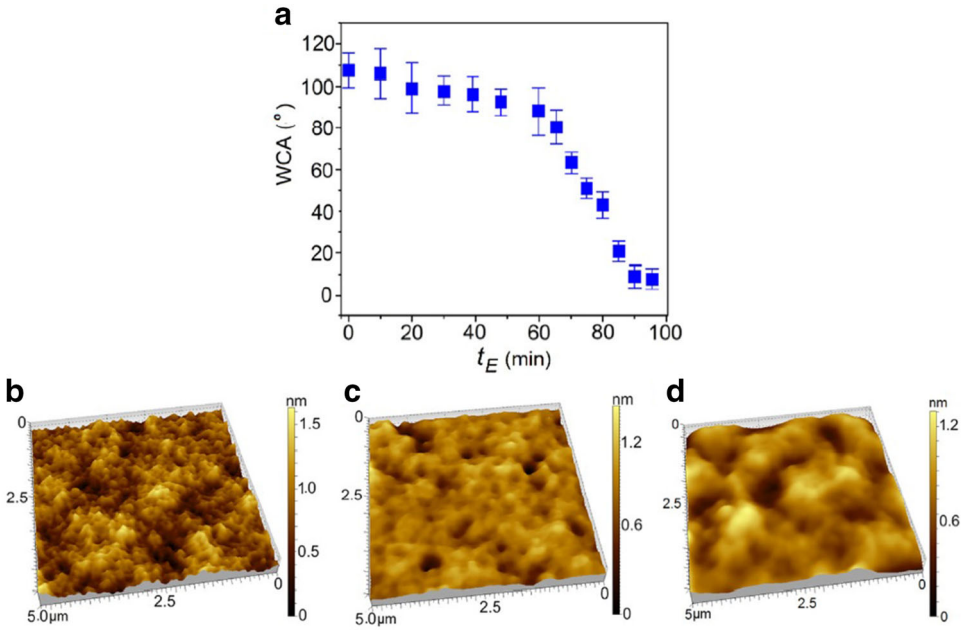

Figure 1. (**a**) Variation in the WCA on Sylgard 184 surface exposed to UVO for different t_E. (**b–d**) AFM image of Sylgard 184 for t_E = 0, 60 and 90 min, respectively.

uncrosslinked PDMS chains to the surface and makes the surface hydrophobic [52–55]. These free siloxane molecules are the intrinsically present uncross linked chains and can also get formed due to UV-induced chain scission reactions [56]. The mechanism of the recovery process as discussed above is shown schematically in figure 2.

Different frames of figure 3 show the progressive hydrophobic recovery of a sample that was initially UVO exposed for $t_E \approx 90$ min, and the ratio of part A to part B is 10:1. It can be seen that the sample exhibits rapid hydrophobic recovery, with a rapid increase in WCA from $\approx 8°$ to $\approx 50°$ within the first 6 h itself. This regime is followed by a sluggish recovery regime between $t_R \approx 6$ h and $t_R \approx 27$ h, when WCA increases from $\approx 50°$ to $\approx 82°$, after which WCA increases only marginally till WCA $\approx$ 89.2° between $t_R \approx 27$ and 200 h. The WCA value remains nearly constant hereafter, which was verified by measuring the WCA on the same sample after 30 days ($t_R \approx 700$ h). This clearly shows that hydrophobic recovery from a stage when the UVO exposed film becomes completely wettable is not 100%, but is limited to $\approx 85\%$ of the initial WCA on the Sylgard sample before subjecting it to UVO exposure.

Figure 4 shows the hydrophobic recovery of samples, which were initially UVO exposed for different durations. In the expected lines, the recovery is more rapid in samples where t_E was low. However, the important aspect is the final recovered value of WCA (which is shown for t_R up to 100 h in figure 4 and remains unaltered till $t_R \approx 200$ h) is different, and expectedly, samples exposed for a lower duration of t_E show higher degree of final recovery of WCA. Importantly, 100% recovery of hydrophobicity is only achieved in samples exposed for t_E lower than 30 min. In all samples exposed for a longer duration, there is some permanent change in the WCA, which can be used advantageously for creating surfaces with tailored hydrophobicity.

Figure 5a and b show the effect of h_F and CL% of the constituent Sylgard 184 film on the extent of hydrophobic recovery on samples that have been subject to the same extent of t_E. It may be observed in both the figures that the initial change or reduction of WCA with t_E remains unaltered irrespective of h_F or CL%. This is expected as UVO exposure only leads to surface modification, and the wettability right after exposure is a function of the thickness and stiffness of the oxide layer, which is obviously the same in all cases. However, as can be seen in figure 5a, the extent of hydrophobic recovery gradually increases with an increase in h_F. As h_F increases, the total volume of the film per unit surface area increases, which means that more number of polymer molecules as well as uncrosslinked chains are present per unit surface area. As a larger number of uncrosslinked chains diffuse towards the surface with time, the extent of hydrophobic recovery is higher in a thicker film. Also, the hydrophobic recovery continues for a longer duration with an increase in h_F. This is because higher h_F leads to a longer path of diffusion for the uncrosslinked chains to reach the top surface. However, the recovery becomes almost independent of film thickness once h_F exceeds ≈ 20 μm. This implies that within the time frame of our measurements, the diffusion length is limited roughly to about 20 μm, and uncrosslinked chains that are at deeper than this depth fails to migrate to the top surface. On the contrary, the recovery becomes sluggish and less when CL% of the film is gradually increased, which can be seen

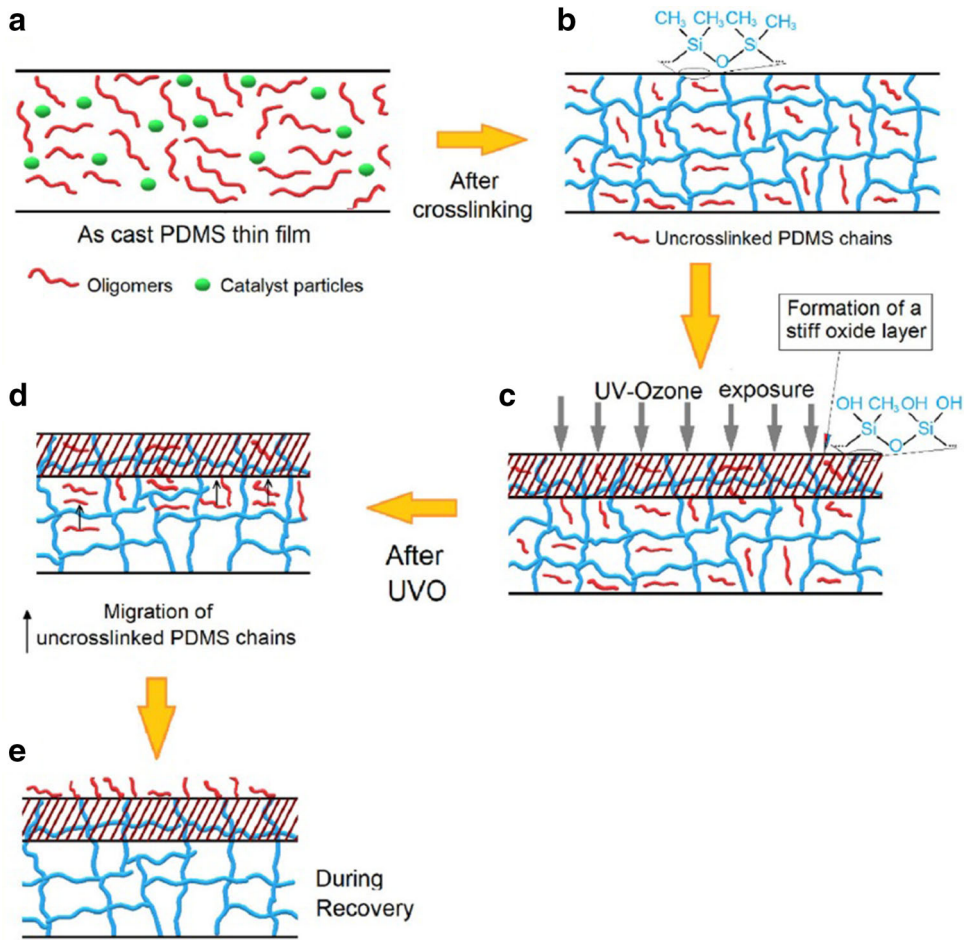

Figure 2. Schematic representing the mechanism of hydrophobic recovery in a PDMS film after UVO exposure.

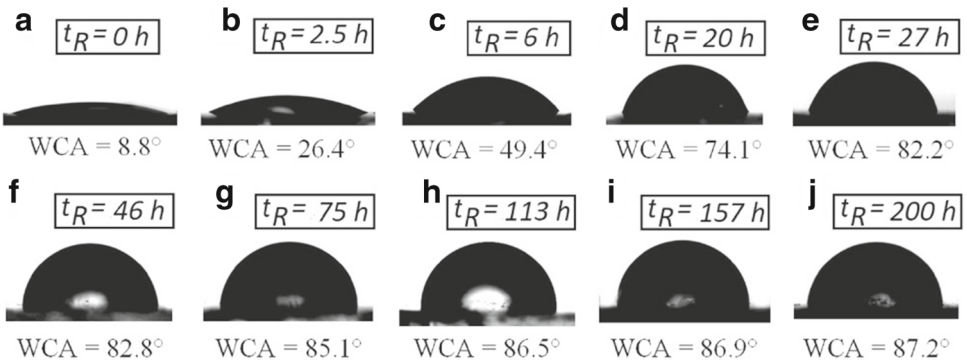

Figure 3. Sequential contact angle goniometer images showing the WCA on surfaces after different durations of recovery time (t_R) for a sample, which was UVO exposed for $t_E \approx 90$ min. The ratio of part A:part B was 10:1 for the sample. The t_R and WCA corresponding to each frame is mentioned in the figure.

in figure 5b. We argue the presence of more part B or cross-linker in the system results in more number of PDMS chains being cross-linked, thereby reducing the availability of uncrosslinked chains that can migrate to the free surface and enhance the hydrophobicity.

Figure 6 shows how the morphology of the replicated patterns get significantly affected by the extent of hydrophobic recovery of a cross-linked UVO-exposed PDMS stamp when the surface of a PS thin film is patterned by capillary force lithography (CFL). In CFL, a technique

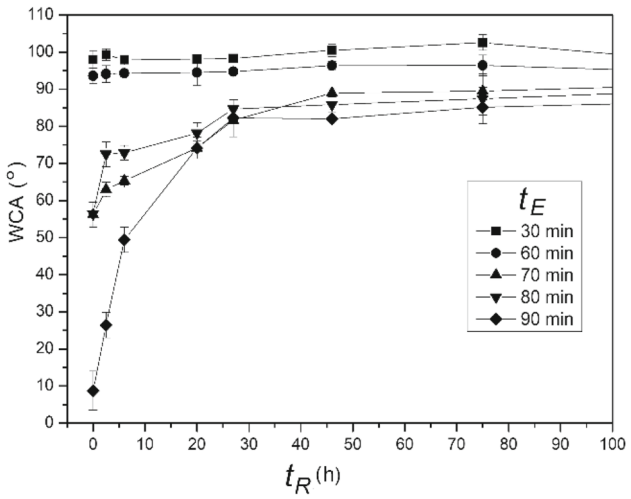

Figure 4. Progressive hydrophobic recovery as a function of recovery time (t_R) for samples exposed to UVO for different durations of t_E. In all cases, the ratio of part A:B was 10:1.

that was pioneered by Lee and co-workers [8], the pattern replication takes place by confined capillary-driven movement of a high viscosity polymer melt, heated above its glass transition temperature along the contours of a stamp which is in conformal contact with the film surface to be patterned. The technique is popular as it does not lead to residual stress accumulation in the patterned structure, which is a perennial problem associated with widely known nano imprint lithography (NIL) [57]. Most nanopatterning techniques aim at creating a perfect negative replica of the original stamp or master, and as Sylgard 184 has low surface energy and does not favour capillary-driven flow of a viscous polymer layer over it during pattern replication, the PDMS stamp is often UVO exposed before bringing in conformal contact with the film surface to be patterned in CFL. It can be seen in figure 6a and e, that by using such a stamp it is indeed possible to obtain a perfect negative replica of a grating patterned stamp and a stamp comprising an array of square pits. In both these cases, the time lag between completion of UVO exposure (t_E = 90 min) and initiation of the pattern replication step is <10 min, and therefore the stamp hardly gets any time to undergo hydrophobic recovery. However, if the time lag between the two steps is gradually increased, it can be seen in frames B–D and frame F of figure 6 that no longer a perfect negative replica is formed, as the stamp surface starts to undergo hydrophobic recovery and therefore the capillarity mediated movement of the polymer layer becomes progressively less favoured.

For the grating patterned stamp, it can be seen that not only the advancing meniscus fails to rise the entire depth of the stamp groove, which is evident from gradual reduction of feature height, from 120 nm for the perfect negative replica down to ~36 nm for a stamp that has been allowed to undergo hydrophobic recovery for 60 h but also fails to fill up the width of the stamp groove, resulting in split type, double periodic structures. Similarly, for a cross patterned stamp, the final pattern morphology comprises an array of square parapets as can be seen in figure 6f, when a stamp that has been allowed to undergo hydrophobic recovery for 50 h is used. Interestingly, for creating the structures shown in figure 6f would have required a much more complex stamp, rather than being a simple array of square pits! Thus, the figure convincingly shows that by suitable modulation of the duration of hydrophobic recovery of the stamp, it becomes possible to create patterns which are no longer limited to a mere negative replica of the original mould or master, thereby providing the possibility of creating patterns on demand using a single master, and keeping all the processing conditions same.

Finally, we discuss a unique application where UVO exposed PDMS blocks are used for patterning another layer

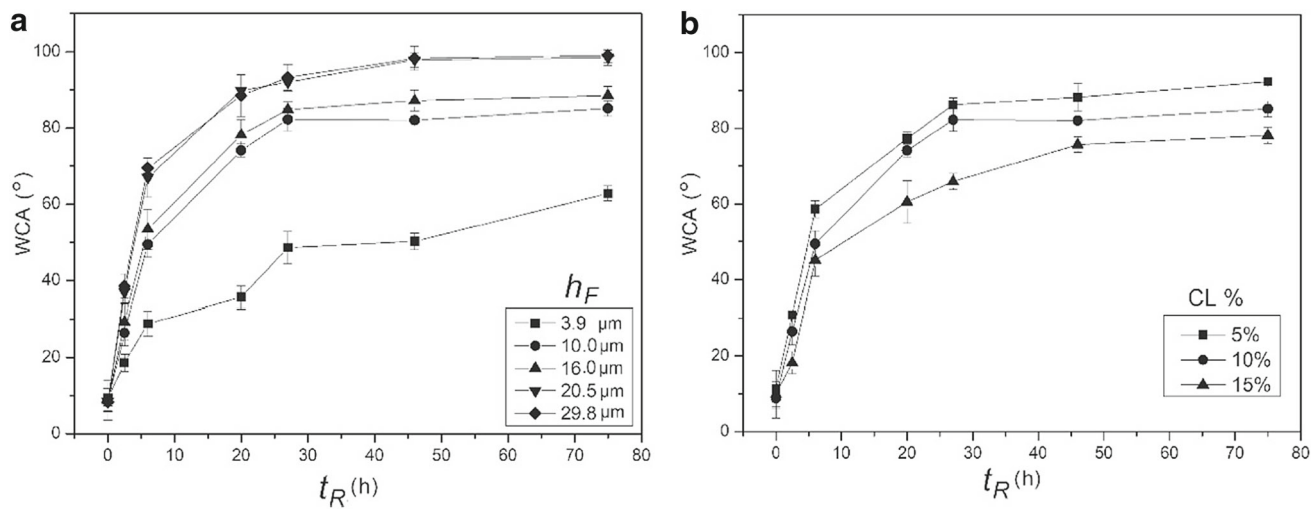

Figure 5. Variation of WCA with t_R for (**a**) different film thickness (h_F) and (**b**) different cross-linker percentage (CL%). In all cases, the films were initially UVO exposed for 90 min. The CL% = 10% in all films of frame A and h_F = 10 µm in all films of frame B.

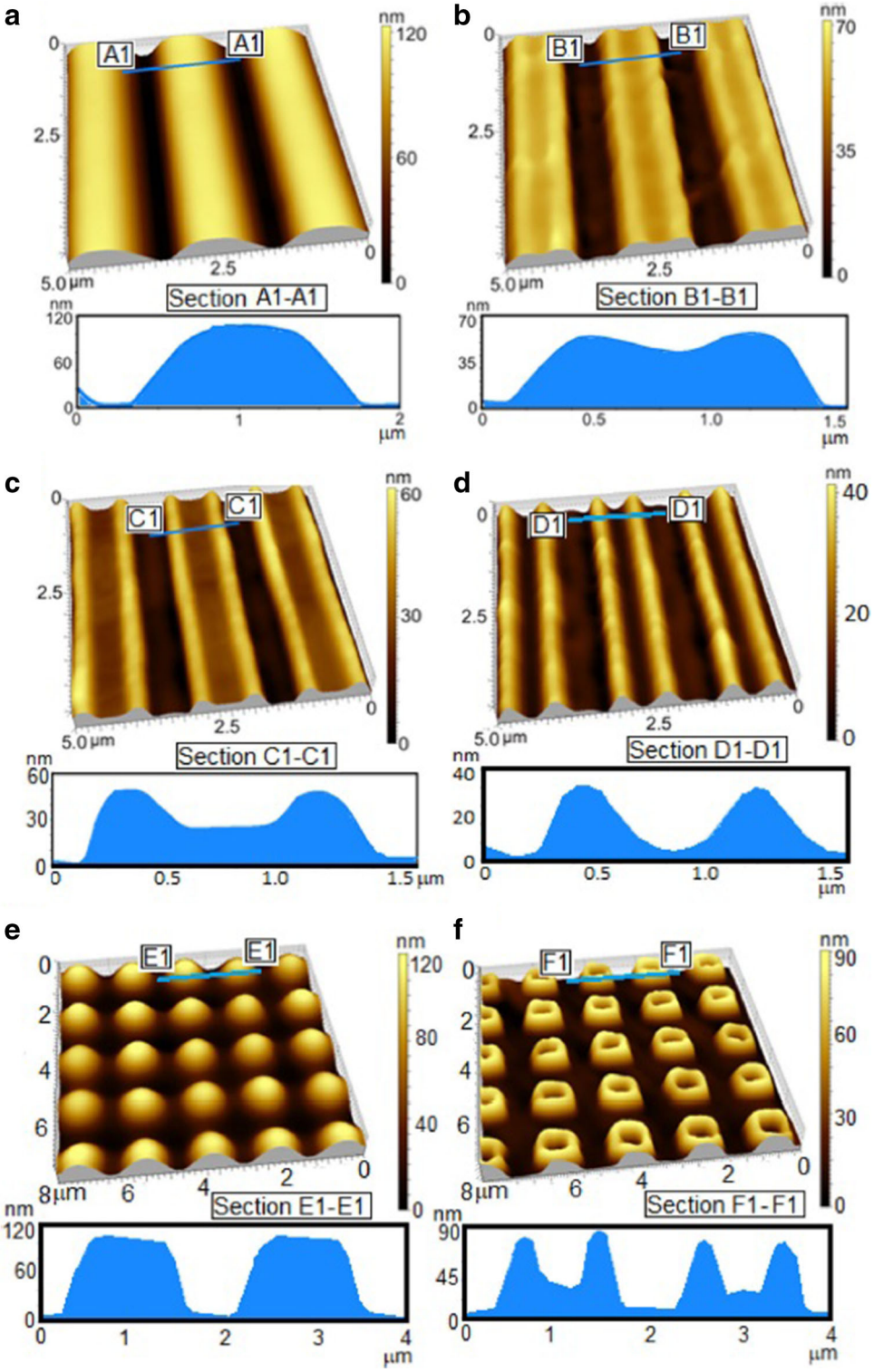

Figure 6. AFM images of PS patterns obtained with Sylgard 184 stamps exposed to UVO for 90 min after the different durations of recovery.

of PDMS film. This particular step is extremely useful in obtaining a positive replica of a biological entity such as a rose petal or a lotus leaf. In most cases, one can easily obtain a negative replica of the biological entity by simple REM. The problem arises while creating the positive replica as cohesive bonding between the stamp and the film to be patterned forms during the thermal cross-linking stage, as both are of the same material. One possible way to

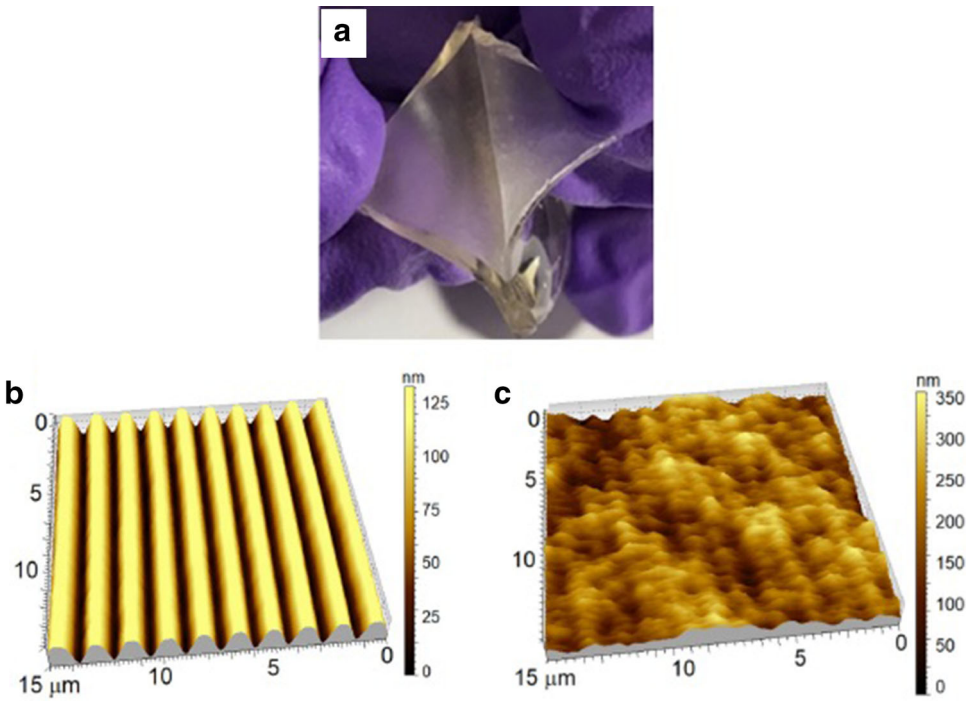

Figure 7. (**a**) Digicam image showing a patterned PDMS film being manually peeled from a cross-linked PDMS stamp. (**b**, **c**) Patterns obtained by replica moulding on the surface of a PDMS film using a PDMS stamp with t_R = 15 min and 6 h, respectively.

overcome this is to use a different polymer for either of the pattern replications steps. However, there are hardly any other candidate materials that can match the effectiveness of Sylgard 184 during REM. This problem of patterning a Sylgard film with a Sylgard stamp has been addressed following tedious protocols such as intermediate metal layer deposition [47] or by using a silica sol–gel film [48] and so on to prevent the cohesive bonding. However, we have shown that it becomes possible to achieve a single step patterning of an uncrosslinked Sylgard 184 film with a Sylgard 184 stamp that has been UVO exposed for 60 min or more [58]. The oxide layer restricts the cohesive bonding between the Sylgard from the stamp and newly poured Sylgard mixture during the second patterning step and after proper thermal annealing, it becomes possible to peel off the Sylgard 184 stamp from the patterned film easily, as can be seen from the digicam image in figure 7a.

What is important to highlight is a perfect negative replica of the stamp pattern following the protocol described above becomes possible to obtain only when t_R is low. For example, figure 7b and c show the morphology of the final patterns when the embossing is done with identical stamps, UVO exposed for t_E = 60 min but with t_R = 15 min and 6 h, respectively. One can clearly see in figure 6b that a neat and perfect negative replica of the original stamp pattern has been obtained when the UVO exposed stamp is allowed to undergo hydrophobic recovery for a short duration. In contrast, when the stamp has been left for a longer duration, the patterned surface is rough and patchy. We argue that the uncrosslinked polymer chains that migrate to the stamp surface come in contact with fresh cross-linked available in the film and get cross-linked at the film–stamp interface causing lumps, hampering the effectiveness of the patterning technique. Thus it becomes evident that hydrophobic recovery plays an important role in patterning a Sylgard film with a UVO exposed Sylgard stamp, which is finding wide application recently, particularly in the context of biomimetic pattern replication [59].

4. Conclusion

In this paper, we have shown modulation of the wettability of a cross-linked PDMS surface by UVO exposure and the effect of subsequent hydrophobic recovery due to migration of the uncrosslinked PDMS chains in the bulk of the film. We have systematically studied the wettability of films after UVO exposure for different durations. We observe that for a film that was completely wettable by about 90 min UVO exposure starts to aggressively recover hydrophobicity within 5 h and subsequently shows a slow recovery to almost 85% of the original contact angle. We also show that the extent of hydrophobic recovery is a function of both film thickness and CL%, where a thicker film with lower CL% exhibits maximum recovery, due to maximization in the number of available uncrosslinked chains. Finally, we also show that UVO exposed PDMS stamps that have undergone different levels of hydrophobic recovery can be used to create patterns that are not a mere negative replica of the original stamp features, due to non-wettability of the stamp

surface engendered by hydrophobic recovery. The hydrophobic recovery can also spoil the possibility of the one-step patterning of PDMS films using a cross-linked UVO exposed PDMS stamp due to cohesive bonding at the film–stamp interface. Therefore, the work highlights the significance of the hydrophobic recovery of UVO exposed PDMS surface in various subsequent applications.

Acknowledgements

NB acknowledges DST INSPIRE Faculty grant (DST/INSPIRE/04/2016/002396). RM acknowledges IMPRINT project (No. 7183) funded by DST and MHRD, Government of India.

References

[1] Sylgard 184 Product Data Sheet, http://www.dowcorning.com/DataFiles/090007b281eb2ada.pdf
[2] Park E J, Sim J K, Jeong M-G, Seo H O and Kim Y D 2013 *RSC Adv.* **3** 12571
[3] Firpo G, Angeli E, Repetto L and Valbusa U 2015 *J. Membr. Sci.* **481** 1
[4] Zuo P, Li X, Dominguez D C and Ye B-C 2013 *Lab Chip* **13** 3921
[5] Chuah Y J, Koh Y T, Lim K, Menon N V, Wu Y and Kang Y 2015 *Sci. Rep.* **5** 18162
[6] Xia Y and Whitesides G M 1998 *Angew. Chem. Int. Ed.* **37** 550
[7] Das A, Banerji A and Mukherjee R 2017 *ACS Appl. Mater. Interfaces* **9** 23255
[8] Suh K Y, Kim Y S and Lee H H 2001 *Adv. Mater.* **13** 1386
[9] Roy R D, Sil D, Jana S, Bhandaru N, Bhadra S K, Biswas P K *et al* 2012 *Ind. Eng. Chem. Res.* **51** 9546
[10] Kumar A and Whitesides G M 1993 *Appl. Phys. Lett.* **63** 2002
[11] Xia Y, Kim E Y, Zhao X M, Rogers J A, Prentiss M and Whitesides G M 1996 *Science* **273** 347
[12] Cayre O, Paunov V N and Velev O D 2003 *J. Mater. Chem.* **13** 2445
[13] Guo L J 2007 *Adv. Mater.* **19** 495
[14] Jeon N L, Hu J, Whitesides G M, Erhardt M K and Nuzzo R G 1998 *Adv. Mater.* **10** 1466
[15] Kung L A, Kam L, Hovis J S and Boxer S G 2000 *Langmuir* **16** 6773
[16] Gorb S N and Scherge M 2000 *Proc. R. Soc. Lond. B* **267** 1239
[17] Varughese S M and Bhandaru N 2019 *Soft Matter* **16** 1692
[18] McDonald J C, Duffy D C, Anderson J R, Chiu D T, Wu H, Schueller O J *et al* 2000 *Electrophoresis* **21** 27
[19] Verma M K S, Majumder A and Ghatak A 2006 *Langmuir* **22** 10291
[20] Dey R, Bhandaru N, Mukherjee R and Chakraborty S 2014 *Soft Matter* **10** 3451
[21] Shull K R, Flanigan C M and Crosby A J 2000 *Phys. Rev. Lett.* **84** 3057
[22] Ghatak A, Chaudhury M K, Shenoy V and Sharma A 2000 *Phys. Rev. Lett.* **85** 4329
[23] Gonuguntla M, Sharma A, Sarkar J, Subramanian S A, Ghosh M and Shenoy V 2006 *Phys. Rev. Lett.* **97** 018303
[24] Sharma A, Gonuguntla M, Mukherjee R, Subramanian S A and Pangule R C 2007 *J. Nanosci. Nanotechnol.* **7** 1744
[25] Mukherjee R and Sharma A 2012 *ACS Appl. Mater. Interfaces* **4** 355
[26] Arun N, Sharma A, Shenoy V B and Narayan K S 2006 *Adv. Mater.* **18** 660
[27] Sahoo S, Bhandaru N and Mukherjee R 2019 *Soft Matter* **15** 3828
[28] Rajput M, Bhandaru N, Anura A, Pal M, Pal B, Paul R R *et al* 2016 *ACS Biomater. Sci. Eng.* **2** 1528
[29] Bhandaru N, Das A, Salunke N and Mukherjee R 2014 *Nano Lett.* **14** 7009
[30] Lee J N, Park C and Whitesides G M 2003 *Anal. Chem.* **75** 6544
[31] Duffy D C, McDonald J C, Schueller O J and Whitesides G M 1998 *Anal. Chem.* **70** 4974
[32] Bernard A, Delamarche E, Schmid H, Michel B, Bosshard H R and Biebuyck H 1998 *Langmuir* **14** 2225
[33] Makamba H, Kim J H, Lim K, Park N and Hahn J H 2003 *Electrophoresis* **24** 3607
[34] Zhou J W, Ellis A V and Voelcker N H 2010 *Electrophoresis* **31** 2
[35] Bhattacharya S, Datta A, Berg J M and Gangopadhyay S 2005 *J. Microelectromech. Syst.* **14** 590
[36] Berdichevsky Y, Khandurina J, Guttman A and Lo Y H 2004 *Sens. Actuators B* **97** 402
[37] Wei K, Rudy M S and Zhao Y 2014 *RSC Adv.* **4** 59122
[38] Hollahan J R and Carlson G L 1970 *J. Appl. Polym. Sci.* **14** 2499
[39] Fritz J L and Owen M J 1995 *J. Adhes.* **54** 33
[40] Olah A, Hillborg H and Vancso G J 2005 *Appl. Surf. Sci.* **239** 410
[41] Efimenko K, Wallace W E and Genzer J 2002 *J. Colloid Interface Sci.* **254** 306
[42] Hillborg H, Tomczak N, Olàh A, Schönherr H and Vancso G J 2004 *Langmuir* **20** 785
[43] Hillborg H, Ankner J F, Gedde U W, Smith G D, Yasuda H K and Wikstrom K 2000 *Polymer* **41** 6851
[44] Senzai T and Fuzikawa S 2019 *Langmuir* **35** 9747
[45] Bhandaru N, Roy S, Harikrishnan G and Mukherjee R 2013 *ACS Macro Lett.* **2** 195
[46] Bhandaru N, Sharma A and Mukherjee R 2016 *ACS Appl. Mater. Interfaces* **9** 19409
[47] Seung-Mo Lee S and Kwon T H 2007 *J. Micromech. Microeng.* **17** 687
[48] Saison T, Peroz C, Chauveau V, Berthier S, Elin Sondergard E and Arribart H 2008 *Bioinsp. Biomim.* **3** 046004
[49] Bhandaru N, Das A and Mukherjee R 2016 *Nanoscale* **8** 1073
[50] Ma K, Rivera J, Hirasaki G J and Biswal S L 2011 *J. Colloid Interface Sci.* **363** 371
[51] Roy S, Ansari K J, Jampa S S K, Vutukuri P and Mukherjee R 2012 *ACS Appl. Mater. Interfaces* **4** 1887
[52] Kim J, Chaudhury M K, Owen M J and Orbeck T J 2001 *Colloid Interface Sci.* **244** 200
[53] Oláh A, Hillborg H and Vancso G J 2005 *Appl. Surf. Sci.* **239** 410

[54] Eddington D T, Puccinelli J P and Beebe D J 2006 *Sens. Actuators B* **114** 170
[55] Kim J, Chaudhury M K and Owen M J 2006 *J. Colloid Interface Sci.* **293** 364
[56] Bodas D and Khan-Malek C 2007 *Sens. Actuators B* **123** 368
[57] Jones R L, Hu T, Soles C L, Lin E K, Reano R M, Pang S W *et al* 2006 *Nano Lett.* **6** 1723
[58] Roy S, Bhandaru N, Das R, Harikrishnan G and Mukherjee R 2014 *ACS Appl. Mater. Interfaces* **6** 6579
[59] Bansal L, Seth P, Sahoo S, Mukherjee R and Basu S 2018 *Appl. Phys. Lett.* **113** 213701